Atomistic simulations of spherical indentations in nanocrystalline gold

D. Feichtinger, P. M. Derlet, and H. Van Swygenhoven
Paul Scherrer Institute, 5232 Villigen, Switzerland
(Received 7 November 2002; published 23 January 2003)

Atomistic simulations are employed to investigate the nanoindentation deformation properties of model nc-Au with grain diameters of 5 and 12 nm, using both conjugant gradient and molecular dynamics. It is found that grain boundaries act as efficient sinks for dislocation nucleation below the indenter and that intergranular sliding occurs. Further, we establish that at the 5-nm grain diameter regime there is a decrease in the Young's modulus.

DOI: 10.1103/PhysRevB.67.024113 PACS number(s): 62.25.+g, 62.20.Fe

The precise nature of the atomic level deformation mechanism in nanocrystalline (nc) materials remains the focus of intense research.[1] Many controversial results have been reported for both the elastic and plastic behaviors of interface-dominated materials. As a function of grain size, the central issue for the elastic regime is the change (if any) in the Young's modulus, and for plasticity, it is the relative degree to which grain boundary sliding (GBS) and dislocation nucleation and propagation contributes as a function of grain size. For the case of nc metals under high uniaxial tensile loading conditions, molecular-dynamics (MD) simulations have provided an atomic level insight into such plastic deformation mechanisms.[2–8] At grain diameters d less than 20 nm, GBS via atomic shuffling (as described in Ref. 9) and stress-assisted free volume migration are found to be the dominant mechanisms[3] at 300 K. More recently, intergranular activity has been observed, such as cooperative GBS in which groups of grains ($d \sim 5$ nm) slide collectively along shear planes extending over a number of grain sizes.[10] In fully three dimensional (3D) nc structures with mean grain sizes above 12 nm, partial dislocations are nucleated at GBs and propagate through the grains, with no full dislocations being observed by us. This is explained by the presence of atomic activity during the emission of the first trailing partial, allowing for the relief of stress in the GB.[5,11] Full dislocations are however observed in a 2D columnar network, where such atomic activity is mainly prohibited due to the 2D restriction.[8]

Nanoindentation offers one of the few experimental techniques to probe in *situ* high strain-rate plasticity at the atomic level.[12,13] Indeed, discrete bursts displayed in experimental load-indentation depth curves have been attributed to the nucleation of individual dislocation events.[14–16] By virtue of this atomic level sensitivity, the role of defects and, more generally, surface inhomogeneities such as surface steps can greatly influence the onset of plasticity.[17] An atomistic simulation therefore provides a natural bridge to complement experimental studies where, for example, it was demonstrated that the structures resulting from onset plasticity are qualitatively similar to that seen in experiments.[18–21] Both MD and conjugate gradient (CG) methods have been used. It is, however, unclear whether some of the reported differences are partly due to the choice of the simulation method. Also, these simulations have all been performed on perfect single-crystal structures. In experiments, however, thin layers are often nc and the resulting onset plasticity may be profoundly affected by the high density of GBs known to interact with lattice dislocations.

In this communication we present an atomistic simulation of nanoindentation into model nc-Au for two samples with average grain diameters of 5 and 12 nm, and compare the results with a simulation for a single-crystal structure. We provide a systematic comparison for results obtained with CG and MD (300 K) methods, and compare the sensitivity of the techniques. The simulations provide three major results: (1) there is a reduction in Young's modulus at the 5-nm-diameter grain size; (2) the surrounding GB structure acts as a sink for the dislocation loops nucleated under the indenter; and (3) for indenter-substrate surface contact areas of less than the grain size, most of the plastic deformation activity is confined within the grain directly below the indenter, whereas for larger contact areas intergranular motion is observed as a result of grain boundary sliding. The simulations also show that full dislocations are possible in a 12-nm grain, stressing the importance of atomic activity during dislocation emission from a nanosized GB.

Nanoindentation simulations were performed on four samples: a single crystal model fcc Au(111) sample (1.1 million atoms), a 12-nm grain size nc-Au sample containing 15 grains (1.2 million atoms) with the grain below the indenter having a (111) surface orientation, and two 5-nm grain size model nc-Au samples containing each 125 grains (800 000 atoms)—one with the grain below the indentor in a (111) surface orientation and the other close to a (123) orientation. The dimensions of all samples are $\sim(26\ \text{nm})^3$. The fully 3D GB networks were prepared using the Voronoi construction,[22] with initially full 3D periodic boundary conditions, similar to the samples used in former work on the GB structure and plastic deformation.[3–5,23,24] The structures were analyzed by using the topological medium-range-order analysis[25] in which, each atom is assigned a crystalline order according to its local environment. In the following figures, gray represents fcc, red represents hcp, green represents 12-coordinated atoms and blue represents non-12 coordinated atoms.

A free-standing thin-film geometry is produced by removing the periodicity along one direction and performing 50 psec of MD at 300 K to allow the surface GB network to find a more equilibrium configuration.[26] During the actual indentation, the bottom layer of atoms was fixed, while periodic boundary conditions were maintained in the lateral direc-

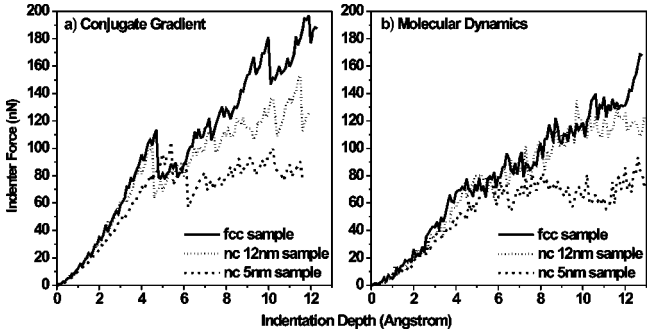

FIG. 1. Load vs indentation depth plots for (a) CG and (b) MD simulation runs.

tions, thereby modeling a thin film residing on a hard substrate.[19–21] For MD, an investigation of the phonon density of states via the velocity-autocorrelation function[27] at the surface region revealed that the vibrational dynamics is not adversely affected by the presence of a fixed layer. A careful equilibration procedure was required to minimize the artificial enhancement of low frequency modes of wavelengths comparable to the indenter film thickness. The second moment potential for Au of Cleri and Rosato[28] was used. In general this potential model underestimates the stacking fault energy when compared to experimental values,[29] and in the case of Au where the experimental stacking fault energy is 30–40 mJ/m^2, the potential underestimates by several tens of mJ/m^2. The spherical indenter was modelled as a strongly repulsive potential $V(r)=A\Theta(R-r)(R-r)^3$ (as in Refs. 19 and 20), where R is the radius of the indenter, r the distance of the indenter center to the atom, A is a force constant, and $\Theta(R-r)$ is the standard step function. Following Ref. 19, R was chosen as 40 Å and A as 5.3 nN/Å^2. In both techniques the indenter was lowered in steps of 0.1 Å. In the case of MD this was performed every 0.5 psec, corresponding to an indentation speed of 20 m/s, which is several orders of magnitude faster than that in experiment but comparable to that used in other MD simulations.[18,30] For the CG simulation, the sample is first cooled to 0 K within the free-standing thin-film geometry with the lateral periodic sample cell lengths following equations of motion derived from a two-dimensional Parinello-Rahman Lagrangian,[31] at which point the fixed bottom layer is introduced. The rational behind employing both CG and MD methods is that the former corresponds to an approximate quasiequilibrium structure obtained by lowering the indenter by small increments, whereas MD at 300 K covers the thermal aspects included in the very early stages of high speed experimental indentations.

Figure 1 displays the force vs. indentation depth curves obtained using CG (a) and MD (b) methods. The CG runs exhibit a distinctive yield point, while the MD runs show significant noise due to temperature effects. The CG yield point for the single crystal is found at a load of 114 nN and an indentation depth of 4.7 Å, which is slightly higher than the ones found for the 12-nm nc sample at 107 nN/4.5 Å and for the 5-nm grain sample at 105 nN/5.4 Å. For the 5-nm sample, an analysis of the atomic structure displayed a plastic deformation before reaching the apparent yield point of the load-indentation depth plot at 5.4 Å. In particular, GB atomic activity and the development of a small stacking fault located in the interface region between the indented grain and a grain below was observed. The elastic modulus calculated by applying the isotropic Hertz model to the appropriate elastic region of each sample, resulted in a (111) Young's modulus of 134 GPa for the single crystal, 129 GPa for the 12-nm sample, and 104 GPa for the 5-nm sample. We note that at zero temperature and pressure $E_{111}=123.8$ GPa for the employed potential.[28] A reduction in the elastic modulus at very small grain sizes was reported many times in literature (see, for example, Ref. 32). Often these results were ascribed to sample artifacts such as pores or impurities in the GBs; however, recently accurate measurements on nc Ni-P samples, with a constant P content, showed a clear drop in Young's modulus for grain diameters in the $\sim$5-nm regime.[33]

Over the plastic part of the CG runs all curves diverge, evidencing the strong influence of the microstructure on the plastic deformation mechanisms. The load-indentation depth curve of the fcc sample shows multiple discrete reductions in load that can be directly related to a discrete dislocation activity involving dislocation nucleation and/or a reorganization of existing dislocation structures. Similar events also take place in the nc samples, but the effect on the load displacement curve is less pronounced, especially in the 5-nm sample, where the active slip plane areas are reduced due to reduced grain size and that intergranular plastic activity is more significant.

The initial CG slip structure, immediately after yield for the single crystal and the 12-nm grain samples, consists of a stacking fault structure roughly of tetrahedral shape with its tip pointing into the sample as seen by Li *et al.*[18] This nearly triaxial symmetry is immediately lost upon a continuation of the indentation, where a complicated succession of partial dislocation reactions leads to a number of dislocation lock structures. All samples exhibit several surface parallel stacking fault planes just below the sample surface. For the MD technique the initial slip led to a wedge-shaped dislocation loop structure in both the single-crystal and 12-nm grain samples, similar to that seen in Refs. 19 and 20. In the 5-nm grain sample, for both the CG and MD methods, the initial slip structure consists of partial dislocations that are immediately attracted to neighboring GBs.

Figure 2 shows the CG atomic structure under the indenter for the single-crystal (a) and the 12-nm grain samples (b) at an indentation depth of $\sim$12 Å. The blue plane of atoms indicates the upper indentation surface. At this indentation depth the dislocation structure remains confined to a compact zone beneath the indenter for the single crystal, whereas for the 12-nm grain sample (b), the initial dislocation loops are attracted to neighboring GBs identified by the green and blue atoms below the surface. Thus the GBs act as dislocation sinks, accommodating the associated slip across the grain by structural changes within the GBs. The inverse process of dislocation nucleation at the GB with associated structural changes in the GB has been observed by us under uniaxial tensile loading conditions.[5]

Recent nanoindentation MD simulations in Al(111) using a free-standing thin-film geometry,[18] demonstrate extended

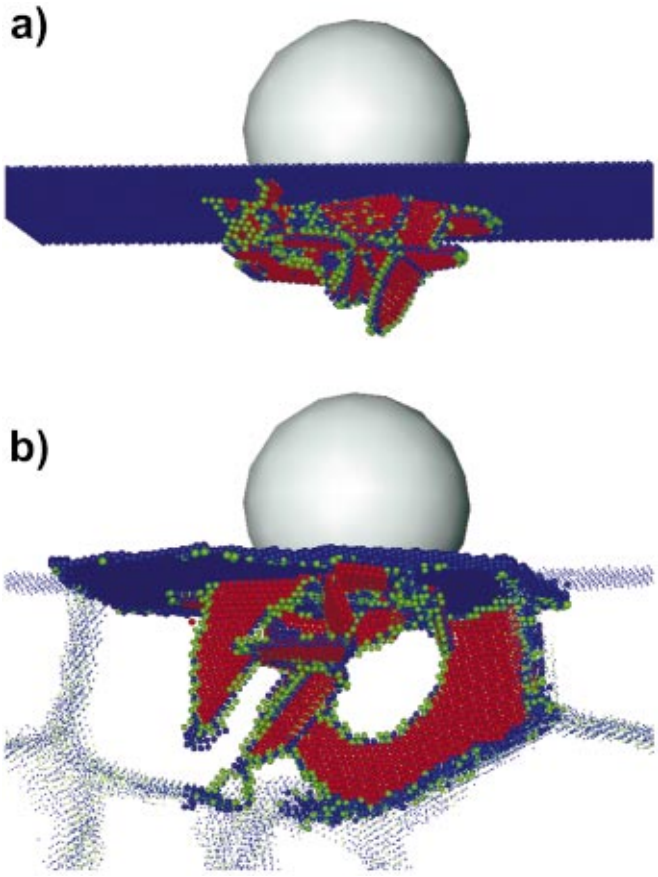

FIG. 2. (Color) Zone beneath the indenter in CG (a) for the single crystal sample at a displacement of 12.3 Å, and (b) for the 12-nm grain sample at a displacement of 11.9 Å. Only non-fcc atoms are shown.

dislocation structures that propagate to the lower surface, contributing in that way to local stress relief, a result that is in contradiction with former observations.[19] Our results suggest that the extent of the dislocations in the Al simulation are a result of the sample geometry in that the free surface acts very similar to the GBs in a nc structure, i.e., by attracting, through ease of accommodation, the emitted dislocation structures. We note that the thickness of the Al(111) thin films is of the order of the diameter of our 12-nm grain size sample.

In Fig. 2(b) an example of a full dislocation in a 12-nm grain is given, where a large stacking fault, which extends throughout the principal grain, is annihilated by a trailing partial dislocation. In our tensile deformation simulations, the lack of a trailing partial (full dislocation) has been ascribed to the structural changes (atomic shuffling and stress assisted migration) observed in the GB during emission of the first partial, allowing stress relaxation and avoiding the immediate need for the emission of the second partial.[5,11] In the present case, partials are emitted below a lowering indenter where local stress is immediately renewed without accommodation by a GB, allowing the trailing partial to be more easily emitted.

In the case of the 5-nm sample where the indenter diameter is larger then the average grain and therefore the indenter-substrate surface area is comparable to the size of the indented grain, the partial dislocation activity extends to neighboring grains and the onset of intergranular motion is observed in the MD run as a result of GBS. The 5-nm grain size sample with the (123) grain orientation below the indenter, was continued to a depth of 20 Å. Figure 3 shows a schematic view of the relative motion of three grains under the indenter, where the largest relative displacement corre-

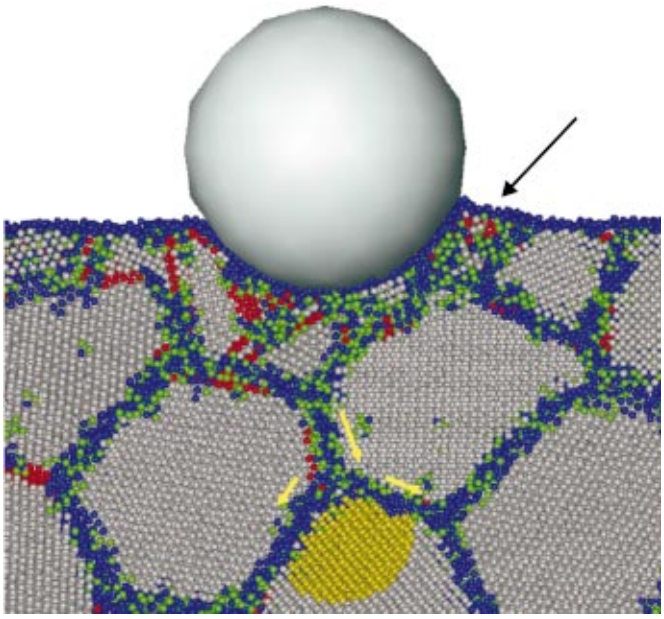

FIG. 3. (Color) A view of the 5-nm average grain size sample at an indentation depth of 20 Å. The yellow arrows signify the relative motion of the grains relative to the center of mass of the yellow atoms.

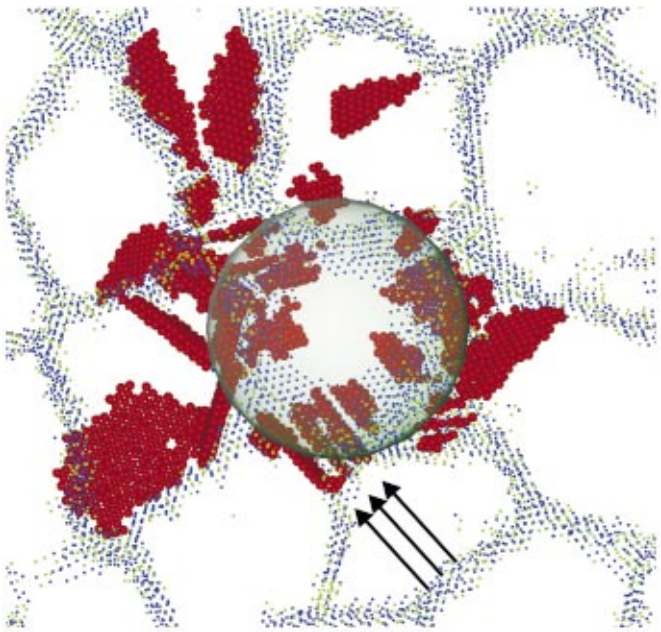

FIG. 4. (Color) Top down view on the stacking fault structure under the indenter of a 5-nm grain size sample illustrating dislocation activity extending into neighboring grains.

sponds to a sliding of about 2 Å along the respective GB. The displacements are relative to those atoms shaded in yellow. Such activity is significantly less in the CG results indicating that GBS is in general facilitated by GB atomic activity such as shuffling and stress-assisted free volume migration—all of which are aided by temperature.[3,34] In this sample some atomic pileup around the indenter is seen (indicated by the black arrow in Fig. 3) with a maximum height of about three atomic layers. This region is highly disordered and may mainly be driven by the high impact velocity of the indenter in the MD simulation. Hence caution should be used in relating this effect to the macroscopic pileup seen in experiment where the active mechanism is generally diffusion limited.

Figure 4 is a top down view illustrating the dislocation activity occurring in adjacent grains, some of which have undergone the GBS identified in Fig. 3. Such associated GB atomic activity has been found to be crucial to the nucleation of dislocations at the GB under uniaxial tensile conditions.[5] The level of local dislocation activity displayed in Fig. 4 is, however, far greater than that seen in previous uniaxial tensile simulations of nc materials, and corresponds to the localized stress gradient around the indenter. Indeed multiple partial dislocation activity within the same grain results in mechanical twinning as indicated by the black arrows in Fig. 4.

In conclusion, our simulations demonstrate the influence of a nc network on nanoindentation curves. For the elastic regime, a decrease in the Young's modulus is observed in the 5-nm grain size sample, and for the plastic regime, two paths for relief of local stress are observed resulting in a softening: (1) GBs act as sinks for the dislocations emitted below the indenter; and (2) when the indenter-substrate surface contact area becomes comparable to the grain size, GBS allows a local grain reorganization. It is also shown that not all observed effects are as clearly reflected by both atomistic simulation methods, MD and CG: elastic effects become more obscured in the MD technique with decreasing grain size, whereas intergranular motion is not so easily observed when the CG method is used.

The authors acknowledge support from the Swiss program TOP NANO 21 (CTI 5443.2).

[1] J.R. Weertman, *Mechanical Behavior of Nanocrystalline Metals, Nanostructured Materials: Processing, Properties and Potential Applications* (Willian Andrew, Norwich, NY, 2002).
[2] H. Van Swygenhoven, M. Spacer, and A. Caro, Acta Mater. **47**, 3117 (1999).
[3] H. Van Swygenhoven and P.M. Derlet, Phys. Rev. B **64**, 224105 (2001).
[4] H. Van Swygenhoven, Science **296**, 66 (2002).
[5] H. Van Swygenhoven, P.M. Derlet, and A. Hasnaoui, Phys. Rev. B **66**, 024101 (2002).
[6] A. Hasnaoui, H. Van Swygenhoven, and P. M. Derlet, Acta Mater. **50**, 3927 (2002).
[7] V. Yamakov, D. Wolf, M. Salazar, S.R. Phillpot, and H. Gleiter, Acta Mater. **49**, 2713 (2001).
[8] V. Yamakov, D. Wolf, S.R. Phillpot, and H. Gleiter, Acta Mater. **50**, 61 (2002).
[9] A. P. Sutton and R. W. Balluffi, *Interfaces in Crystalline Materials* (Oxford Science Publications, Oxford, 1996).
[10] A. Hasnaoui, H. Van Swygenhoven, and P.M. Derlet, Phys. Rev. B **66**, 184112 (2002).
[11] P. M. Derlet and H. Van Swygenhoven, Scr. Mater. **47**, 719 (2002).
[12] W.W. Gerberich, J.C. Nelson, E.T. Lilleoddem, P. Anderson, and J.T. Wryobek, Acta Mater. **44**, 3585 (1996).
[13] P. Tangyunyong, R.C. Thomas, J.E. Houston, T.A. Michalske, R.M. Crooks, and A.J. Howard, Phys. Rev. Lett. **71**, 3319 (1993).
[14] A. Gouldstone, H.-J. Koh, K.-Y. Zeng, A.E. Giannakopoulos, and S. Suresh, Acta Mater. **48**, 2277 (2000).
[15] S.G. Corcoran, S.R. Brankovic, N. Dimitrov, and K. Sieradzki, in *Thin-Films–Stresses and Mechanical Properties VII*, edited by R.C. Cammarata, E.P. Busso, M. Nastasi, and W.C. Oliver, MRS Symposia Proceedings No. 505 (Materials Research Society, Pittsburgh, 1998).
[16] J. de la Figuera, M.A. Gonzáles, R. García-Martínez, J.M. Rojo, O.S. Hernán, A.L. Vásquez de Parga, and R. Miranda, Phys. Rev. B **58**, 1169 (1998).
[17] J.D. Kiely, R.Q. Hwang, and J.E. Houston, Phys. Rev. Lett. **81**, 4424 (1998).
[18] J. Li, K.J. Van Vliet, T. Zhi, S. Yip, and S. Suresh, Nature (London) **418**, 307 (2002).
[19] C.L. Kelchner, S.J. Plimpton, and J.C. Hamilton, Phys. Rev. B **58**, 11 085 (1998).
[20] J.A. Zimmermann, C.L. Kelchner, P.A. Klein, J.C. Hamilton, and S.F. Foiles, Phys. Rev. Lett. **87**, 165507 (2001).
[21] O.R. de la Fuente, J.A. Zimmerman, M.A. Gonzalez, J. de la Figuera, J.C. Hamilton, W.W. Pei, and J.M. Rojo, Phys. Rev. Lett. **88**, 036101 (2002).
[22] G.Z. Voronoi, J. Reine Angew. Math. **134**, 199 (1908).
[23] H. Van Swygenhoven and A. Caro, Phys. Rev. B **58**, 11 246 (1998).
[24] H. Van Swygenhoven, D. Farkas, and A. Caro, Phys. Rev. B **62**, 831 (2000).
[25] J.D. Honeycutt and H.C. Andersen, J. Phys. Chem. **91**, 4950 (1987).
[26] P.M. Derlet and H. Van Swygenhoven, Philos. Mag. A **82**, 1 (2001).
[27] P.M. Derlet, R. Meyer, J.L. Lewis, U. Stuhr, and H. Van Swygenhoven, Phys. Rev. Lett. **87**, 205501 (2001).
[28] F. Cleri and V. Rosato, Phys. Rev. B **48**, 22 (1993).
[29] R. Meyer and L.J. Lewis, Phys. Rev. B **66**, 052106 (2002).
[30] D. Christopher, R. Smith, and A. Richter, Nanotechnology **12**, 372 (2001).
[31] M. Parrinello and A. Rahman, J. Appl. Phys. **52**, 7182 (1981).
[32] G.W. Nieman and J.R. Weertman, J. Mater. Res. **6**, 1012 (1991).
[33] Y. Zhou, U. Erb, K.T. Aust, and G. Palumbo (unpublished).
[34] H. Van Swygenhoven, M. Spaczer, A. Caro, and D. Farkas, Phys. Rev. B **60**, 22 (1999).